JOURNAL OF GUIDANCE, CONTROL, AND DYNAMICS
Vol. 20, No. 6, November–December 1997

# Minimum Model Error Approach for Attitude Estimation

John L. Crassidis*
*Catholic University of America, Washington, D.C. 20064*
and
F. Landis Markley†
*NASA Goddard Space Flight Center, Greenbelt, Maryland 20771*

**An optimal batch estimator and smoother based on the minimum model error (MME) approach is developed for three-axis stabilized spacecraft. The formulation is shown using only attitude sensors, e.g., three-axis magnetometers, sun sensors, star trackers. This algorithm accurately estimates the attitude of a spacecraft and substantially smoothes noise associated with attitude sensor measurements. The general functional form of the optimal estimation approach involves the solution of a nonlinear two-point-boundary-value problem that can be solved only by using computationally intense methods. A linearized solution also is shown that is computationally more efficient than methods that solve the general form. The linearized solution is useful when an a priori estimate of the angular velocity is already known, which can be obtained from a finite difference of a determined attitude, or from propagation of a dynamics model. Results using this new algorithm indicate that an MME-based approach accurately estimates the attitude of an actual spacecraft with the sole use of magnetometer sensor measurements.**

## Introduction

THE attitude of a spacecraft can be determined either by deterministic methods or by utilizing algorithms that combine dynamic and/or kinematic models with sensor data. Three-axis deterministic methods, such as TRIAD,[1] QUEST,[2] and FOAM,[3] require at least two sets of vector measurements to determine the attitude. An advantage of both the QUEST and FOAM algorithms is that the attitude of a spacecraft can be estimated using more than two sets of measurements. This is accomplished by minimizing a quadratic loss function first posed by Wahba.[4] However, all deterministic methods fail when only one set of vector measurements is available, e.g., magnetometer data only. Estimation algorithms utilize dynamic and/or kinematic models, and subsequently can (in theory) estimate the attitude of a spacecraft using only one set of vector measurements. Although all spacecraft in use today have at least two onboard attitude sensors, estimation techniques can be used to determine the attitude during anomalous periods, such as solar eclipses and/or sensor coalignment.

The most commonly used technique for attitude estimation is the Kalman filter.[5] The Kalman filter utilizes state-space representations to both estimate plant dynamics and filter noisy data. Errors in the dynamical model and measurement process are assumed to be modeled by a zero-mean Gaussian process with known covariance. The optimality criterion in the Kalman filter minimizes the trace error covariance between estimated responses and true responses. Smoothing algorithms further refine state estimates by utilizing both a forward filter and a backward filter.[6] An advantage of smoothing algorithms is that the error covariance is always less than or equal to either the forward or the backward filter alone. A disadvantage of smoothing algorithms is that they cannot be implemented in sequential (real-time) estimation.

Early practical applications of Kalman filtering for attitude estimation are given by Pauling et al.[7] and Toda et al.[8] for the Space Precision Attitude Reference System. In particular, Pauling et al.[7] used the now-familiar quaternion representation for model prediction in the filter design. Because the quaternion representation is free of singularities (thus avoiding the gimbal-lock situation) and because the attitude matrix is algebraic in the quaternion components, this representation is used most frequently in attitude determination and estimation algorithms. A more complete survey of other attitude representations is given by Shuster.[9] Also, a more complete survey of early Kalman filtering techniques for attitude estimation is given by Lefferts et al.[10]

More recent studies using Kalman filtering techniques have been performed for the Earth Radiation Budget Satellite (ERBS),[11,12] the Upper Atmospheric Research Satellite,[13] the Extreme Ultra Violet Explorer (EUVE),[14] and the Solar Anomalous Magnetospheric Particle Explorer (SAMPEX).[15,16] In particular, studies of the EUVE spacecraft involved the application of a smoothing algorithm to further reduce errors in the estimated attitudes using both attitude sensors and gyro data. Also, studies of both the ERBS and SAMPEX spacecraft used Kalman filtering techniques for attitude estimation that involved gyro degradation or gyro omission. The thrust of all of these investigations is to improve attitude estimates through the use of optimally tuned filter parameters, thereby providing the means for reliable backup attitude estimation schemes.

For spacecraft attitude estimation, the Kalman filter is most applicable to spacecraft equipped with three-axis gyros as well as attitude sensors.[10] However, gyros generally are expensive and often are prone to degradation or failure. Therefore, in recent years, gyros have been omitted, e.g., in Small Explorer spacecraft, such as SAMPEX. To circumvent the problem of gyro omission or failure, analytical models of rate motion can be used. This approach has been successfully used in a real-time sequential filter (RTSF) algorithm, which propagates state estimates and error covariances using dynamic models.[16] The estimation of dynamic rates by the RTSF is accomplished from angular momentum model propagation and then correcting for these rates by using a gyro bias component in the filter design. A clear advantage of using dynamic models is shown for the case of near coalignment of the spacecraft-to-sun and magnetic-field vectors. For this case, deterministic algorithms, such as TRIAD and QUEST, show anomalous behaviors with extreme deviations in determined attitudes. Because the RTSF propagates an analytical model of motion, attitude estimates are available even when data from only one attitude sensor are available. However, fairly accurate models of control and disturbance torques were required to obtain accurate estimates.[16]

Although the quaternion representation is the most commonly used for attitude estimation, the problem of maintaining proper normalization exists. This constraint leads to a singularity in the covariance matrix, which, in actual practice, is difficult to maintain because

Received June 22, 1995; revision received July 14, 1997; accepted for publication July 16, 1997. 

*Assistant Professor, Department of Mechanical Engineering. Senior Member AIAA.

†Staff Engineer, Guidance, Navigation, and Control Branch, Code 712. Associate Fellow AIAA.

of linearization and/or computer roundoff error. Three solutions (two of which yield identical results) to this problem are summarized by Lefferts et al.[10] The first approach uses the transition matrix of the state-error vector to obtain a reduced-order representation of the error covariance. The second approach deletes one of the quaternion components to obtain a truncated error covariance expression. The third approach uses an incremental quaternion error, which results in a representation that is identical to the first approach. This approach is most commonly used to maintain normalization for the estimated quaternion.

Bar-Itzhack and Deutschmann[12] show two further approaches to quaternion normalization. The first approach represents the state vector by additive corrections to the quaternion estimated by the Kalman filter. However, this approach does not maintain the normalization constraint unless it converges to the correct quaternion.[12] Renormalization is carried out externally to the Kalman filter. This approach can be useful in obtaining a faster convergence but lacks physical sense in the filter's state propagation. The second approach uses the normalized quaternion as a pseudomeasurement. The renormalization subsequently is carried out by performing a measurement update ideally with zero noise on the pseudomeasurement, thereby forcing the estimated quaternion to the normalized quaternion. However, attitude solutions converge to incorrect values when noise levels are high.[12]

In this paper, an optimal attitude estimation and smoothing algorithm is developed that is capable of accurate state estimation for spacecraft lacking accurate or any gyro measurements and/or accurate dynamic models. This algorithm is based on the minimum model error (MME)[17] batch-estimation approach. The advantages of the MME estimator over conventional Kalman strategies include the following. 1) No a priori statistics on the form of the model error are required. 2) The actual model error is determined as part of the solution. 3) The state estimates are always free of jump discontinuities. For quaternion estimation, the MME nonlinear estimator has the additional advantage that quaternion normalization is maintained as an inherent feature of the process. The MME estimation approach has been applied successfully to numerous poorly modeled dynamic systems that exhibit highly nonlinear behaviors, e.g., see Refs. 18 and 19.

Initial results obtained by use of an MME approach to estimate the attitude and angular rates of SAMPEX utilized TRIAD-determined attitudes as measurements.[20,21] The formulation expands upon this technique to use attitude sensors, such as three-axis magnetometers (TAM), fine sun sensors (FSS), and star trackers. The general functional form of the optimal estimation approach involves the solution of a nonlinear two-point-boundary-value problem (TPBVP). This problem has been solved previously by using gradient-based techniques.[22] However, gradient-based techniques can be computationally intense. The MME-based approach utilizes a linearization technique similar to that in Ref. 10 with a Riccati transformation. This leads to an algorithm that is easy to design and implement in actual practice.

Organization of this paper proceeds as follows. First, a summary of the spacecraft attitude kinematics, dynamics, and sensor models is given. Then, a brief review of the MME estimator for nonlinear systems is given. Next, an MME-based estimator is developed for the purpose of attitude estimation. A general attitude estimation formulation is shown that uses the nonlinear kinematics and dynamics model. Then, a linearization technique with a Riccati transformation is derived to provide a computationally efficient algorithm. Finally, to demonstrate the usefulness of this algorithm, the MME estimator is used to estimate the attitude of SAMPEX.

## Attitude Kinematics and Dynamics

In this section, a brief review of the kinematic and dynamic equations of motion for a three-axis stabilized spacecraft is given. The attitude is assumed to be represented by the quaternion, defined as

$$\boldsymbol{q} \equiv \begin{bmatrix} \boldsymbol{q}_{13} \\ q_4 \end{bmatrix} \tag{1}$$

with

$$\boldsymbol{q}_{13} \equiv \begin{bmatrix} q_1 \\ q_2 \\ q_3 \end{bmatrix} = \hat{\boldsymbol{n}} \sin\left(\frac{\theta}{2}\right) \tag{2a}$$

$$q_4 = \cos(\theta/2) \tag{2b}$$

where $\hat{\boldsymbol{n}}$ is a unit vector corresponding to the axis of rotation and $\theta$ is the angle of rotation. The quaternion kinematic equations of motion are derived by using the spacecraft's angular velocity ($\boldsymbol{\omega}$), given by

$$\dot{\boldsymbol{q}}(t) = \tfrac{1}{2}\Omega(\boldsymbol{\omega})\,\boldsymbol{q}(t) = \tfrac{1}{2}\Xi(\boldsymbol{q})\,\boldsymbol{\omega}(t) \tag{3}$$

where $\Omega(\boldsymbol{\omega})$ and $\Xi(\boldsymbol{q})$ are defined as

$$\Omega(\boldsymbol{\omega}) \equiv \begin{bmatrix} -[\boldsymbol{\omega}\times] & \vdots & \boldsymbol{\omega} \\ \cdots\cdots\cdots & \vdots & \cdots \\ -\boldsymbol{\omega}^T & \vdots & 0 \end{bmatrix} \tag{4a}$$

$$\Xi(\boldsymbol{q}) \equiv \begin{bmatrix} q_4 I_{3\times 3} + [\boldsymbol{q}_{13}\times] \\ \cdots\cdots\cdots\cdots\cdots \\ -\boldsymbol{q}_{13}^T \end{bmatrix} \tag{4b}$$

The $3\times 3$ dimensional matrices $[\boldsymbol{\omega}\times]$ and $[\boldsymbol{q}_{13}\times]$ are referred to as cross-product matrices because $\boldsymbol{a}\times\boldsymbol{b} = [\boldsymbol{a}\times]\boldsymbol{b}$, with

$$[\boldsymbol{a}\times] \equiv \begin{bmatrix} 0 & -a_3 & a_2 \\ a_3 & 0 & -a_1 \\ -a_2 & a_1 & 0 \end{bmatrix} \tag{5}$$

The quaternion obeys the following normalization constraint:

$$\boldsymbol{q}^T\boldsymbol{q} = \boldsymbol{q}_{13}^T\boldsymbol{q}_{13} + q_4^2 = 1 \tag{6}$$

Also, the matrix $\Xi(\boldsymbol{q})$ obeys the following helpful relations:

$$\Xi^T(\boldsymbol{q})\Xi(\boldsymbol{q}) = \boldsymbol{q}^T\boldsymbol{q} I_{3\times 3} \tag{7a}$$

$$\Xi(\boldsymbol{q})\Xi^T(\boldsymbol{q}) = \boldsymbol{q}^T\boldsymbol{q} I_{4\times 4} - \boldsymbol{q}\boldsymbol{q}^T \tag{7b}$$

$$\Xi^T(\boldsymbol{q})\boldsymbol{q} = \boldsymbol{0}_{3\times 1} \tag{7c}$$

$$\Xi^T(\boldsymbol{q})\,\boldsymbol{\lambda} = -\Xi^T(\boldsymbol{\lambda})\boldsymbol{q} \qquad \text{for any} \qquad \boldsymbol{\lambda}_{4\times 1} \tag{7d}$$

The measurement model is assumed to be of the form

$$\boldsymbol{B}_B = A(\boldsymbol{q})\boldsymbol{B}_I \tag{8}$$

where $\boldsymbol{B}_I$ is a $3\times 1$ dimensional vector of some reference object, e.g., a vector to the sun or to a star or the Earth's magnetic-field vector, in a reference coordinate system; $\boldsymbol{B}_B$ is a $3\times 1$ dimensional vector defining the components of the corresponding reference vector measured in the spacecraft body frame; and $A(\boldsymbol{q})$ is given by

$$A(\boldsymbol{q}) = \left(q_4^2 - \boldsymbol{q}_{13}^T\boldsymbol{q}_{13}\right) I_{3\times 3} + 2\boldsymbol{q}_{13}\boldsymbol{q}_{13}^T - 2q_4[\boldsymbol{q}_{13}\times] \tag{9}$$

which is the $3\times 3$ dimensional (orthogonal) attitude matrix.

The dynamic equations of motion, also known as Euler's equations, for a rotating spacecraft[23] are given by

$$\dot{\boldsymbol{L}}(t) = \boldsymbol{N}(t) - \boldsymbol{\omega}(t)\times\boldsymbol{L}(t) \tag{10}$$

where $\boldsymbol{L}$ is the total angular momentum; $\boldsymbol{N}$ is the total external torque, which includes, e.g., control torques, aerodynamic drag torques, solar pressure torques; and $J$ is the inertia matrix of the spacecraft. If reaction or momentum wheels are used on the spacecraft, the total angular momentum is given by

$$\boldsymbol{L}(t) = J\boldsymbol{\omega}(t) + \boldsymbol{h}(t) \tag{11}$$

where $\boldsymbol{h}$ is the total angular momentum due to the wheels. Thus, Eq. (10) can be rewritten as

$$\dot{\boldsymbol{L}}(t) = \boldsymbol{N}(t) - \{J^{-1}[\boldsymbol{L}(t) - \boldsymbol{h}(t)]\}\times\boldsymbol{L}(t) \tag{12}$$

Also, from Eqs. (10) and (11), the following angular-velocity form of Euler's equation can be used:

$$J\dot{\boldsymbol{\omega}}(t) = \boldsymbol{N}(t) - \dot{\boldsymbol{h}}(t) - \boldsymbol{\omega}(t) \times [J\boldsymbol{\omega}(t) + \boldsymbol{h}(t)] \tag{13}$$

which involves the derivative of the wheel angular momentum.

## MME Estimation

In this section, a brief review of the MME estimation algorithm is given. The essential feature of this batch estimator is that actual model error trajectories are determined during the estimation process, unlike most filter/smoother algorithms, which assume that the model error is a stochastic process with known properties. The MME algorithm determines the correction added to the assumed model, which yields an accurate representation of the system's behavior. This is accomplished by solving an optimality condition using an output residual constraint. Therefore, accurate state estimates can be determined without the use of precise system representations in the assumed model.

The MME algorithm assumes that the state estimates are given by a preliminary model and a to-be-determined model-error vector, given by

$$\dot{\hat{\boldsymbol{x}}}(t) = \boldsymbol{f}[\hat{\boldsymbol{x}}(t), \boldsymbol{u}(t), \boldsymbol{d}(t), t] \tag{14a}$$

$$\hat{\boldsymbol{y}}(t) = \boldsymbol{g}[\hat{\boldsymbol{x}}(t), t] \tag{14b}$$

where $\boldsymbol{f}$ is an $n \times 1$ model vector, $\hat{\boldsymbol{x}}(t)$ is an $n \times 1$ state-estimate vector, $\boldsymbol{u}(t)$ is a $p \times 1$ vector of known inputs, $\boldsymbol{d}(t)$ is an $l \times 1$ model-error vector, $\boldsymbol{g}$ is a $q \times 1$ measurement vector, and $\hat{\boldsymbol{y}}(t)$ is a $q \times 1$ estimated-output vector. State-observable discrete measurements are assumed for Eq. (14b) in the following form:

$$\tilde{\boldsymbol{y}}(t_k) = \boldsymbol{g}_k[\boldsymbol{x}(t_k), t_k] + \boldsymbol{\nu}_k \tag{15}$$

where $\tilde{\boldsymbol{y}}(t_k)$ is a $q \times 1$ measurement vector at time $t_k$; and $\boldsymbol{\nu}_k$ is a $q \times 1$ measurement-noise vector, which is assumed to be a zero-mean, Gaussian distributed process with known covariance.

In the MME algorithm, the optimal state estimates are determined on the basis that the measurement-minus-estimate error covariance matrix must match the measurement-minus-truth error covariance matrix. This condition is referred to as the covariance constraint, shown as

$$\{\tilde{\boldsymbol{y}}(t_k) - \boldsymbol{g}_k[\hat{\boldsymbol{x}}(t_k), t_k]\}\{\tilde{\boldsymbol{y}}(t_k) - \boldsymbol{g}_k[\hat{\boldsymbol{x}}(t_k), t_k]\}^T = R_k \tag{16}$$

where $R_k$ is the element-by-element (known) measurement-error covariance. However, problems may arise using Eq. (16), which are attributed to small-sample statistics.[24] Therefore, in the typical case in which the measurement-error process is stationary, the average covariance can be used, given by

$$\frac{1}{m}\sum_{k=1}^{m}\{\tilde{\boldsymbol{y}}(t_k) - \boldsymbol{g}_k[\hat{\boldsymbol{x}}(t_k), t_k]\}\{\tilde{\boldsymbol{y}}(t_k) - \boldsymbol{g}_k[\hat{\boldsymbol{x}}(t_k), t_k]\}^T \approx R \tag{17}$$

where $m$ is the total number of measurements.

Next, the following cost function is minimized with respect to $\boldsymbol{d}(\tau)$:

$$J = \frac{1}{2}\sum_{k=1}^{m}\{\tilde{\boldsymbol{y}}(t_k) - \boldsymbol{g}_k[\hat{\boldsymbol{x}}(t_k), t_k]\}^T R^{-1}\{\tilde{\boldsymbol{y}}(t_k) - \boldsymbol{g}_k[\hat{\boldsymbol{x}}(t_k), t_k]\} + \frac{1}{2}\int_{t_0}^{t_f} \boldsymbol{d}^T(\tau) W \boldsymbol{d}(\tau)\, \mathrm{d}\tau \tag{18}$$

where $W$ is an $n \times n$ positive-definite weighting matrix. The necessary conditions for the minimization of $J$ lead to the following TPBVP[17]:

$$\dot{\hat{\boldsymbol{x}}}(t) = \boldsymbol{f}[\hat{\boldsymbol{x}}(t), \boldsymbol{u}(t), \boldsymbol{d}(t), t] \tag{19a}$$

$$\boldsymbol{d}(t) = -W^{-1}\left[\frac{\partial \boldsymbol{f}}{\partial \boldsymbol{d}}\right]^T \boldsymbol{\lambda}(t) \tag{19b}$$

$$\dot{\boldsymbol{\lambda}}(t) = -\left[\frac{\partial \boldsymbol{f}}{\partial \hat{\boldsymbol{x}}}\right]^T \boldsymbol{\lambda}(t) \tag{19c}$$

$$\boldsymbol{\lambda}\left(t_k^+\right) = \boldsymbol{\lambda}\left(t_k^-\right) + H^T(t_k)\{\tilde{\boldsymbol{y}}(t_k) - \boldsymbol{g}_k[\hat{\boldsymbol{x}}(t_k), t_k]\} \tag{19d}$$

$$H(t_k) \equiv \left.\frac{\partial \boldsymbol{g}}{\partial \hat{\boldsymbol{x}}}\right|_{\hat{\boldsymbol{x}}(t_k), t_k} \tag{19e}$$

where $\boldsymbol{\lambda}(t)$ is an $n \times 1$ costate vector that is updated at each measurement point using Eq. (19d). The boundary conditions are selected such that either $\boldsymbol{\lambda}(t_0^-) = \boldsymbol{0}$ or $\hat{\boldsymbol{x}}(t_0)$ is specified at the initial time and either $\boldsymbol{\lambda}(t_f^+) = \boldsymbol{0}$ or $\hat{\boldsymbol{x}}(t_f)$ is specified at the final time.

## Attitude Estimation

In this section, the MME estimator is derived for spacecraft that lack any rate information. First, a general MME-based algorithm using the nonlinear kinematics and dynamics equations of motion is shown. Next, a linearized algorithm with a Riccati-type transformation is derived using an a priori estimate of the angular velocity.

### General Formulation

The general formulation is based on use of Euler's equation for modeling the angular momentum and the quaternion kinematics equation for the attitude. The MME problem for this case minimizes the following cost function:

$$J = \frac{1}{2}\sum_{k=1}^{m}\{\tilde{\boldsymbol{B}}_B - A(\hat{\boldsymbol{q}})\boldsymbol{B}_I\}^T\Big|_{t_k} R^{-1}\{\tilde{\boldsymbol{B}}_B - A(\hat{\boldsymbol{q}})\boldsymbol{B}_I\}\Big|_{t_k} + \frac{1}{2}\int_{t_0}^{t_f} \boldsymbol{d}^T(\tau) W \boldsymbol{d}(\tau)\, \mathrm{d}\tau \tag{20}$$

subject to

$$\begin{bmatrix}\dot{\hat{\boldsymbol{q}}}(t)\\ \dot{\hat{\boldsymbol{L}}}(t)\end{bmatrix} = \begin{bmatrix}\frac{1}{2}\Omega(\hat{\boldsymbol{\omega}}) & 0_{4\times 3}\\ 0_{3\times 4} & -[\hat{\boldsymbol{\omega}}\times]\end{bmatrix}\begin{bmatrix}\hat{\boldsymbol{q}}(t)\\ \hat{\boldsymbol{L}}(t)\end{bmatrix} + \begin{bmatrix}0_{4\times 3}\\ I_{3\times 3}\end{bmatrix}\boldsymbol{N}(t) + \begin{bmatrix}0_{4\times 3}\\ I_{3\times 3}\end{bmatrix}\boldsymbol{d}(t), \qquad \begin{bmatrix}\hat{\boldsymbol{q}}(t_0)\\ \hat{\boldsymbol{L}}(t_0)\end{bmatrix} = \begin{bmatrix}\hat{\boldsymbol{q}}_0\\ \hat{\boldsymbol{L}}_0\end{bmatrix} \tag{21}$$

where

$$\hat{\boldsymbol{\omega}} = J^{-1}\{\hat{\boldsymbol{L}} - \tilde{\boldsymbol{h}}\} \tag{22}$$

$\tilde{\boldsymbol{h}}$ is the measured angular momentum due to the wheels, and $\tilde{\boldsymbol{B}}$ denotes the body measurement. Note that the model-error term $\boldsymbol{d}$ acts as a torque model correction to the dynamics. Minimizing Eq. (20) leads to the TPBVP given by Eqs. (21) and the following:

$$\boldsymbol{d}(t) + W^{-1}\boldsymbol{\lambda}_L(t) = \boldsymbol{0} \tag{23a}$$

$$\begin{bmatrix}\dot{\boldsymbol{\lambda}}_q(t)\\ \dot{\boldsymbol{\lambda}}_L(t)\end{bmatrix} = \begin{bmatrix}\frac{1}{2}\Omega(\hat{\boldsymbol{\omega}}) & 0_{4\times 3}\\ -\frac{1}{2}J^{-1}\Xi^T(\hat{\boldsymbol{q}}) & -[\hat{\boldsymbol{\omega}}\times] + J^{-1}[\hat{\boldsymbol{L}}\times]\end{bmatrix}\begin{bmatrix}\boldsymbol{\lambda}_q(t)\\ \boldsymbol{\lambda}_L(t)\end{bmatrix}, \qquad \boldsymbol{\lambda}_L(t_f) = \boldsymbol{0} \tag{23b}$$

with discrete jumps in the costates given by

$$\boldsymbol{\lambda}_q\left(t_k^+\right) = \boldsymbol{\lambda}_q\left(t_k^-\right) + H^T(\boldsymbol{l})R^{-1}\{\tilde{\boldsymbol{B}}_B - A(\hat{\boldsymbol{q}})\boldsymbol{B}_I\}\Big|_{t_k}, \qquad \boldsymbol{\lambda}_q\left(t_f^+\right) = \boldsymbol{0} \tag{24}$$

The matrix $H$ in Eqs. (24) can be derived to be

$$H(\boldsymbol{l}) = 2\Xi^T(\boldsymbol{l}) \tag{25}$$

where

$$\boldsymbol{l} = \Psi(\hat{\boldsymbol{q}})\boldsymbol{B}_I \tag{26a}$$

$$\Psi(\hat{\boldsymbol{q}}) \equiv \begin{bmatrix}-\hat{q}_4 I_{3\times 3} + [\hat{\boldsymbol{q}}_{13}\times]\\ \cdots\cdots\cdots\cdots\\ \hat{\boldsymbol{q}}_{13}^T\end{bmatrix} \tag{26b}$$

The TPBVP given by Eqs. (21) and (23) can be solved by using a simple gradient-based search technique. The extension to multiple attitude sensors is accomplished by using a partitioned residual output and sensitivity matrix, given by

$$\begin{bmatrix} H_1^T & \cdots & H_{m_{\text{tot}}}^T \end{bmatrix} \begin{bmatrix} \left\{\tilde{\boldsymbol{B}}_{B_1} - A(\hat{\boldsymbol{q}})\boldsymbol{B}_{I_1}\right\} \\ \vdots \\ \left\{\tilde{\boldsymbol{B}}_{B_{m_{\text{tot}}}} - A(\hat{\boldsymbol{q}})\boldsymbol{B}_{I_{m_{\text{tot}}}}\right\} \end{bmatrix} \tag{27}$$

where $m_{\text{tot}}$ is the total number of vector observations. Note that the MME state estimate in Eqs. (21) is free of jump discontinuities, unlike traditional smoothing algorithms such as the Kalman smoother.

The costate update in Eqs. (24) shows a nonlinear relationship with respect to the quaternion estimate. However, this nonlinearity can be reduced to a linear function if the quaternions obey normalization and the measurement errors are assumed to be isotropic, i.e., equal for each axis so that $R = r I_{3\times 3}$, where $r$ is a scalar. This can be shown by deriving the costate update using

$$\frac{1}{2r}\frac{\partial}{\partial \hat{\boldsymbol{q}}}\left\{[\tilde{\boldsymbol{B}}_B - A(\hat{\boldsymbol{q}})\boldsymbol{B}_I]^T[\tilde{\boldsymbol{B}}_B - A(\hat{\boldsymbol{q}})\boldsymbol{B}_I]\right\} \tag{28}$$

To determine the partial derivative in Eq. (28), the following identities and definitions are used:

$$E(\boldsymbol{B}_I) \equiv \begin{bmatrix} -[\boldsymbol{B}_I\times] & \vdots & -\boldsymbol{B}_I \\ \cdots\cdots\cdots & \vdots & \cdots \\ \boldsymbol{B}_I^T & \vdots & 0 \end{bmatrix} \tag{29a}$$

$$A(\hat{\boldsymbol{q}}) = -\Xi^T(\hat{\boldsymbol{q}})\Psi(\hat{\boldsymbol{q}}) \tag{29b}$$

$$\Psi(\hat{\boldsymbol{q}})\boldsymbol{B}_I = E(\boldsymbol{B}_I)\hat{\boldsymbol{q}} \tag{29c}$$

$$E(\boldsymbol{B}_I)E(\boldsymbol{B}_I) = -I_{4\times 4}\boldsymbol{B}_I^T\boldsymbol{B}_I \tag{29d}$$

Equation (28) now can be rewritten as

$$\frac{1}{2r}\frac{\partial}{\partial \hat{\boldsymbol{q}}}\left\{\tilde{\boldsymbol{B}}_B^T\tilde{\boldsymbol{B}}_B - 2\hat{\boldsymbol{q}}^T\Omega(\tilde{\boldsymbol{B}}_B)E(\boldsymbol{B}_I)\hat{\boldsymbol{q}} + \left(\boldsymbol{B}_I^T\boldsymbol{B}_I\right)(\hat{\boldsymbol{q}}^T\hat{\boldsymbol{q}})^2\right\} \tag{30}$$

The partial derivative in Eq. (30) is given by

$$(2/r)\left\{-\Omega(\tilde{\boldsymbol{B}}_B)E(\boldsymbol{B}_I)\hat{\boldsymbol{q}} + \left(\boldsymbol{B}_I^T\boldsymbol{B}_I\right)(\hat{\boldsymbol{q}}^T\hat{\boldsymbol{q}})\hat{\boldsymbol{q}}\right\} \tag{31}$$

Hence, if the quaternions obey normalization, the following identity is true:

$$\Xi(\boldsymbol{I})\{\tilde{\boldsymbol{B}}_B - A(\hat{\boldsymbol{q}})\boldsymbol{B}_I\} = \left\{\Omega(\tilde{\boldsymbol{B}}_B)E(\boldsymbol{B}_I) - \left(\boldsymbol{B}_I^T\boldsymbol{B}_I\right)I_{4\times 4}\right\}\hat{\boldsymbol{q}} \tag{32}$$

Therefore, if the sensor measurement errors are isotropic, the costate update in Eq. (24) is linear with respect to the quaternion estimate. Equation (32) also leads to another useful identity:

$$\Xi(\boldsymbol{I}) = E(\boldsymbol{B}_I)\Xi(\boldsymbol{q}) \tag{33}$$

**Linearized Formulation**

The linearized method involves a two-step process. The first determines the angular velocity using a simplified MME cost function and a nominal angular velocity input. The second uses the MME-determined angular velocity to determine a torque model error correction. Although the second step is not required for an attitude solution, it may be useful in providing a correction to the dynamics model for linear and/or nonlinear identification.[21] The MME attitude angular velocity estimation formulation minimizes the following cost function:

$$J = \frac{1}{2}\sum_{k=1}^{m}\{\tilde{\boldsymbol{B}}_B - A(\hat{\boldsymbol{q}})\boldsymbol{B}_I\}^T\Big|_{t_k} R^{-1}\{\tilde{\boldsymbol{B}}_B - A(\hat{\boldsymbol{q}})\boldsymbol{B}_I\}\Big|_{t_k} + \frac{1}{2}\int_{t_0}^{t_f}\boldsymbol{d}^T(\tau)W\boldsymbol{d}(\tau)\,\mathrm{d}\tau \tag{34}$$

subject to

$$\dot{\hat{\boldsymbol{q}}}(t) = \tfrac{1}{2}\Omega[\boldsymbol{d}_n(t) + \boldsymbol{d}(t)]\hat{\boldsymbol{q}}(t), \qquad \hat{\boldsymbol{q}}(t_0) = \hat{\boldsymbol{q}}_0 \tag{35}$$

where $\boldsymbol{d}_n$ is an a priori estimate of the angular velocity. The model error ($\boldsymbol{d}$) is now a correction to the nominal angular velocity. The TPBVP for this problem is given by

$$\dot{\hat{\boldsymbol{q}}}(t) = \tfrac{1}{2}\Omega[\boldsymbol{d}_n(t) + \boldsymbol{d}(t)]\hat{\boldsymbol{q}}(t), \qquad \hat{\boldsymbol{q}}(t_0) = \hat{\boldsymbol{q}}_0 \tag{36a}$$

$$\boldsymbol{d}(t) = -\tfrac{1}{2}W^{-1}\Xi^T(\hat{\boldsymbol{q}})\,\boldsymbol{\lambda}(t) \tag{36b}$$

$$\dot{\boldsymbol{\lambda}}(t) = \tfrac{1}{2}\Omega[\boldsymbol{d}_n(t) + \boldsymbol{d}(t)]\,\boldsymbol{\lambda}(t) \tag{36c}$$

$$\boldsymbol{\lambda}\left(t_k^+\right) = \boldsymbol{\lambda}\left(t_k^-\right) + H^T(\boldsymbol{I})R^{-1}\{\tilde{\boldsymbol{B}}_B - A(\hat{\boldsymbol{q}})\boldsymbol{B}_I\}\Big|_{t_k}, \qquad \boldsymbol{\lambda}\left(t_f^+\right) = \boldsymbol{0} \tag{36d}$$

A linearized solution can be derived by using error quaternion multiplication; this approach is similar to the linear equations used in Ref. 10. First, define an error quaternion given [dropping the ($t$) notation for now] by

$$\delta\hat{\boldsymbol{q}} = \hat{\boldsymbol{q}} \otimes \boldsymbol{q}_n^{-1} \tag{37}$$

where $\delta\hat{\boldsymbol{q}}$ is the error quaternion and $\boldsymbol{q}_n$ is a nominal quaternion determined using $\boldsymbol{d}_n$. The inverse quaternion is determined by taking the negative of the first three components. The quaternion product is defined as

$$\boldsymbol{q}_a \otimes \boldsymbol{q}_b \equiv \left[\Xi(\boldsymbol{q}_b) \;\vdots\; \boldsymbol{q}_b\right]\boldsymbol{q}_a \tag{38}$$

Taking the time derivative of Eq. (37) yields

$$\delta\dot{\hat{\boldsymbol{q}}} = \dot{\hat{\boldsymbol{q}}} \otimes \boldsymbol{q}_n^{-1} + \hat{\boldsymbol{q}} \otimes \dot{\boldsymbol{q}}_n^{-1} \tag{39}$$

Substituting the quaternion kinematic equations into Eq. (39) gives

$$\delta\dot{\hat{\boldsymbol{q}}} = \frac{1}{2}\begin{bmatrix}\boldsymbol{d}\\0\end{bmatrix} \otimes \delta\hat{\boldsymbol{q}} - \frac{1}{2}\delta\hat{\boldsymbol{q}} \otimes \begin{bmatrix}\boldsymbol{d}_n\\0\end{bmatrix} \tag{40}$$

Equation (40) can be rewritten as

$$\delta\dot{\hat{\boldsymbol{q}}} = \frac{1}{2}\left\{\begin{bmatrix}\boldsymbol{d}_n\\0\end{bmatrix} \otimes \delta\hat{\boldsymbol{q}} - \delta\hat{\boldsymbol{q}} \otimes \begin{bmatrix}\boldsymbol{d}_n\\0\end{bmatrix}\right\} + \frac{1}{2}\begin{bmatrix}\delta\boldsymbol{d}\\0\end{bmatrix} \otimes \delta\hat{\boldsymbol{q}} \tag{41}$$

where

$$\delta\boldsymbol{d} = \boldsymbol{d} - \boldsymbol{d}_n \tag{42}$$

If $\delta\hat{\boldsymbol{q}}_4 \approx 1$, then second-order terms in Eq. (41) are negligible and the fourth derivative error component is zero, which leads to

$$\delta\dot{\hat{\boldsymbol{q}}}_{13} = -[\boldsymbol{d}_n\times]\delta\hat{\boldsymbol{q}}_{13} + \tfrac{1}{2}\delta\boldsymbol{d} \tag{43}$$

with

$$\delta\hat{\boldsymbol{q}}_{13} = \Xi^T(\boldsymbol{q}_n)\hat{\boldsymbol{q}} \tag{44}$$

To determine $\delta\boldsymbol{d}$, the cost function in Eq. (34) is minimized subject to the equality constraint in Eq. (43). This minimization leads to the following TPBVP:

$$\delta\dot{\hat{\boldsymbol{q}}}_{13}(t) = -[\boldsymbol{d}_n(t)\times]\delta\hat{\boldsymbol{q}}_{13}(t) - \tfrac{1}{2}\boldsymbol{d}_n(t) - \tfrac{1}{4}W^{-1}\boldsymbol{\lambda}(t), \qquad \delta\hat{\boldsymbol{q}}_{13}(t_0) = \boldsymbol{0} \tag{45a}$$

$$\dot{\boldsymbol{\lambda}}(t) = -[\boldsymbol{d}_n(t)\times]\,\boldsymbol{\lambda}(t) \tag{45b}$$

$$\boldsymbol{\lambda}\left(t_k^+\right) = \boldsymbol{\lambda}\left(t_k^-\right) - 2[A(\boldsymbol{q}_n)\boldsymbol{B}_I\times]R^{-1}\{\tilde{\boldsymbol{B}}_B - A(\boldsymbol{q}_n)\boldsymbol{B}_I - 2[A(\boldsymbol{q}_n)\boldsymbol{B}_I\times]\delta\hat{\boldsymbol{q}}_{13}\}\Big|_{t_k}, \qquad \boldsymbol{\lambda}\left(t_f^+\right) = \boldsymbol{0} \tag{45c}$$

The TPBVP in Eqs. (45) can be decoupled by introducing a time-varying Riccati transformation.[25] This leads to the following set of equations:

$$\dot{P}(t) = P(t)[\boldsymbol{d}_n(t)\times] + [\boldsymbol{d}_n(t)\times]^T P(t) + \tfrac{1}{4}P(t)W^{-1}P(t) \quad (46a)$$

$$P\left(t_k^-\right) = P\left(t_k^+\right) - 4[A(\boldsymbol{q}_n)\boldsymbol{B}_I\times]R^{-1}[A(\boldsymbol{q}_n)\boldsymbol{B}_I\times]\Big|_{t_k}$$

$$P\left(t_f^+\right) = 0 \quad (46b)$$

$$\dot{z}(t) = \left\{\tfrac{1}{4}P(t)W^{-1} - [\boldsymbol{d}_n(t)\times]\right\}z(t) + \tfrac{1}{2}P(t)\boldsymbol{d}_n(t) \quad (46c)$$

$$z\left(t_k^-\right) = z\left(t_k^+\right) + 2[A(\boldsymbol{q}_n)\boldsymbol{B}_I\times]R^{-1}\tilde{\boldsymbol{B}}_B\Big|_{t_k}, \qquad z\left(t_f^+\right) = \boldsymbol{0} \quad (46d)$$

Therefore, the Riccati trajectories in Eq. (46a) are integrated backward in time with discrete updates given at the measurement time by Eq. (46b). Also, the inhomogeneous trajectories in Eq. (46c) are integrated backward in time accounting for discrete jumps by use of Eq. (46d). Then, the error quaternion trajectories can be solved by integrating the following equation forward in time:

$$\delta\dot{\hat{\boldsymbol{q}}}_{13}(t) = -\left\{[\boldsymbol{d}_n(t)\times] + \tfrac{1}{4}W^{-1}P(t)\right\}\delta\hat{\boldsymbol{q}}_{13}(t) - \tfrac{1}{2}\boldsymbol{d}_n(t) - \tfrac{1}{4}W^{-1}\boldsymbol{z}(t), \qquad \delta\hat{\boldsymbol{q}}_{13}(t_0) = \boldsymbol{0} \quad (47)$$

The estimated quaternion trajectories then can be constructed by using

$$\hat{\boldsymbol{q}} = \begin{bmatrix} \delta\hat{\boldsymbol{q}}_{13} \\ 1 \end{bmatrix} \otimes \boldsymbol{q}_n \quad (48)$$

The MME angular rate trajectories $\boldsymbol{\omega} = \boldsymbol{d}_n + \boldsymbol{d}$ in Eq. (35) now can be used to estimate model error torques. First, a measured angular momentum vector is determined by

$$\tilde{\boldsymbol{L}} = J\boldsymbol{\omega} + \tilde{\boldsymbol{h}} \quad (49)$$

In general, the angular momentum measurements in Eq. (49) will be noisy because of the measurements of the wheel speed. However, this noise can be smoothed by another simple linear MME estimator.[22] The MME problem for determining the errors in the torque input of Euler's equation minimizes the following cost function:

$$J = \frac{1}{2}\sum_{k=1}^{m}\{\tilde{\boldsymbol{L}}(t) - \hat{\boldsymbol{L}}(t)\}^T\Big|_{t_k} R^{-1}\{\tilde{\boldsymbol{L}}(t) - \hat{\boldsymbol{L}}(t)\}\Big|_{t_k} + \frac{1}{2}\int_{t_0}^{t_f}\boldsymbol{d}^T(\tau)W\boldsymbol{d}(\tau)\,\mathrm{d}\tau \quad (50)$$

subject to

$$\dot{\hat{\boldsymbol{L}}}(t) = -[\boldsymbol{\omega}(t)\times]\hat{\boldsymbol{L}}(t) + \boldsymbol{N}(t) + \boldsymbol{d}(t), \qquad \hat{\boldsymbol{L}}(t_0) = \hat{\boldsymbol{L}}_0 \quad (51)$$

The matrix $R$ in Eq. (50) now represents the covariance of the noise associated with $\tilde{\boldsymbol{L}}$. Minimizing Eq. (50) leads to the following TPBVP:

$$\dot{\hat{\boldsymbol{L}}}(t) = -[\boldsymbol{\omega}(t)\times]\hat{\boldsymbol{L}}(t) + \boldsymbol{N}(t) - W^{-1}\boldsymbol{\lambda}(t), \qquad \hat{\boldsymbol{L}}(t_0) = \hat{\boldsymbol{L}}_0 \quad (52a)$$

$$\dot{\boldsymbol{\lambda}}(t) = -[\boldsymbol{\omega}(t)\times]\boldsymbol{\lambda}(t) \quad (52b)$$

$$\boldsymbol{\lambda}\left(t_k^+\right) = \boldsymbol{\lambda}\left(t_k^-\right) + R^{-1}\{\tilde{\boldsymbol{L}} - \hat{\boldsymbol{L}}\}\Big|_{t_k}, \qquad \boldsymbol{\lambda}\left(t_f^+\right) = \boldsymbol{0} \quad (52c)$$

The solution to the TPBVP in Eq. (52) also can be found by using a Riccati transformation, which leads to the following equations:

$$\dot{P}(t) = P(t)[\boldsymbol{\omega}(t)\times] + [\boldsymbol{\omega}(t)\times]^T P(t) + P(t)W^{-1}P(t) \quad (53a)$$

$$P\left(t_k^-\right) = P\left(t_k^+\right) + R^{-1}, \qquad P\left(t_f^+\right) = 0 \quad (53b)$$

$$\dot{z}(t) = \{P(t)W^{-1} - [\boldsymbol{\omega}(t)\times]\}z(t) - P(t)\boldsymbol{N}(t) \quad (53c)$$

$$z\left(t_k^-\right) = z\left(t_k^+\right) + R^{-1}\tilde{\boldsymbol{L}}\Big|_{t_k}, \qquad z\left(t_f^+\right) = \boldsymbol{0} \quad (53d)$$

$$\dot{\hat{\boldsymbol{L}}}(t) = \{-[\boldsymbol{\omega}(t)\times] - W^{-1}P(t)\}\hat{\boldsymbol{L}}(t) - W^{-1}z(t) + \boldsymbol{N}(t), \qquad \hat{\boldsymbol{L}}(t_0) = \hat{\boldsymbol{L}}_0 \quad (53e)$$

Therefore, the Riccati and inhomogeneous trajectories are solved backward in time by use of Eqs. (53a) and (53c), accounting for discrete jumps by Eqs. (53b) and (53d). Then, the angular momentum estimates are determined by integrating Eq. (53e) forward in time.

**Attitude Estimation of an Actual Spacecraft**

In this section, the MME attitude estimation algorithm previously developed is used to estimate the attitude, rates, and torque modeling errors of the SAMPEX spacecraft with magnetometer data only. The spacecraft is three-axis stabilized in a 550 × 675 km elliptical orbit with an 82-deg inclination. A schematic of the spacecraft with axis definitions is shown in Fig. 1. The spacecraft is nominally controlled to rotate about the $y$ axis at some constant rate; the other axis rates are controlled to near zero. The attitude-control hardware consists of a magnetic torquer assembly (MTA) and a single reaction wheel. The attitude-determination hardware consists of five coarse sun sensors, primarily for sun acquisition, one FSS, and a TAM. No rate gyroscopic instruments are present on the spacecraft.

The onboard computer routine to determine attitude is based on the TRIAD[1] deterministic method. The spacecraft is controlled by the MTA to maintain the fixed solar arrays perpendicular to the sun line. The reaction wheel is used to point the instrument boresight axis as required by the scientific mission. During eclipse, no sun measurements are available from the FSS. Attitude control is maintained by using a constant sunline vector as a pseudomeasurement. The MTA is turned off during eclipse, but the reaction wheel is still used to control pitch. During vector coalignment, the spacecraft is placed in a coast mode, in which neither the MTA nor the reaction wheel is used (see Ref. 26 for more details). The required nominal attitude-determination accuracy is ±2 deg. During anomalous conditions (eclipse and/or measurement-vector coalignment), an accurate attitude cannot be determined by deterministic methods such as TRIAD. The MME algorithm can determine the attitude using TAM measurements only, so that attitude accuracy can be checked for any deviations from nominal performance.

The inertial magnetic field is obtained by using an eighth-order spherical harmonic model of the Earth's magnetic field with International Geomagnetic Reference Field coefficients. Magnetometer measurements by the TAM are known to be extremely accurate (within 0.3 mG). However, experience has shown that errors in the magnetic-field model have a standard deviation of about 3 mG

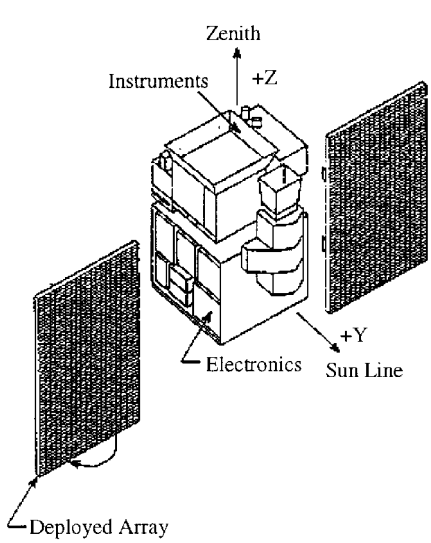


**Fig. 1 SAMPEX spacecraft.**

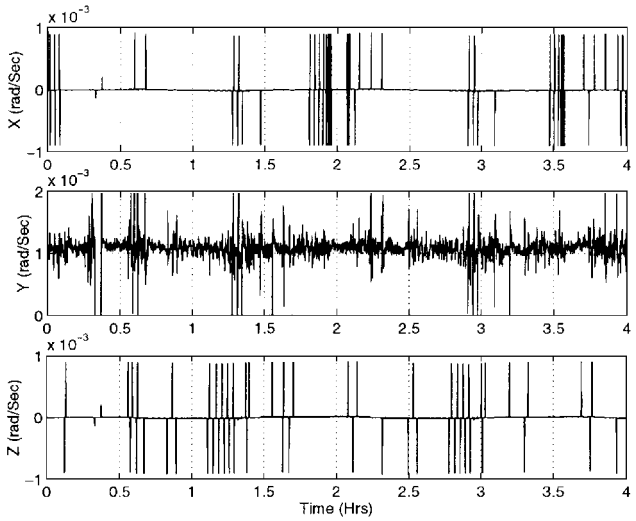


**Fig. 2 Plot of TRIAD-determined angular velocities.**

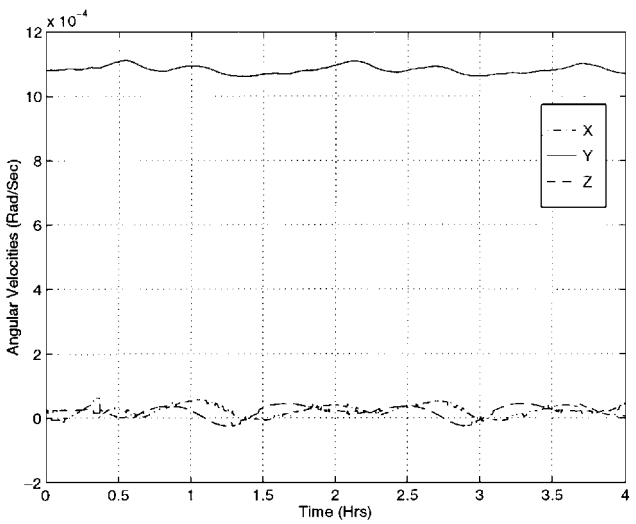


**Fig. 3 Plot of MME-determined angular velocities.**

(Ref. 16). Therefore, 9 $mG^2$ is chosen for the diagonal elements of the measurement covariance matrix.

A plot of the angular velocities determined by taking finite differences of the TRIAD attitude solutions is shown in Fig. 2. These rates are extremely noisy, which is due to the large digitization noise associated with the FSS measurements. Also, the large errors at the beginning are due to a TAM outage or loss of signal. To demonstrate the MME capabilities, a test case was run using only TAM measurements to estimate the attitude and angular rates. The linearized MME estimator is implemented using Eqs. (46–48) with the angular velocities shown in Fig. 2 as the nominal estimates. The weighting matrix is determined by using a simple parameter optimization scheme with a quadratic form of the covariance constraint as a cost function. A plot of the MME-determined angular velocities is shown in Fig. 3. This plot clearly shows a rotation about the spacecraft $y$ axis, which is the desired control motion. Also, a noticeable motion in the $x$ and $z$ axes is evident, which is not easily seen in Fig. 2. This motion may be due to the MTA not fully damping spacecraft nutation. Although this is not relevant for the SAMPEX spacecraft (because requirements are not stringent), it clearly shows the capability of the MME estimator to significantly smooth the noise associated with the available sensor complement. A plot of the error between the estimated MME attitudes using TAM data only and the attitudes determined by TRIAD is shown in Fig. 4. A slight hangoff is seen in the pitch axis. This may be due to nonlinear effects in the magnetic-field model. Although the accuracy using TAM cannot be fully known for this system, the methodology of the MME approach seems to provide a reasonable method for attitude estimation, while performing substantial smoothing of noisy measurements.

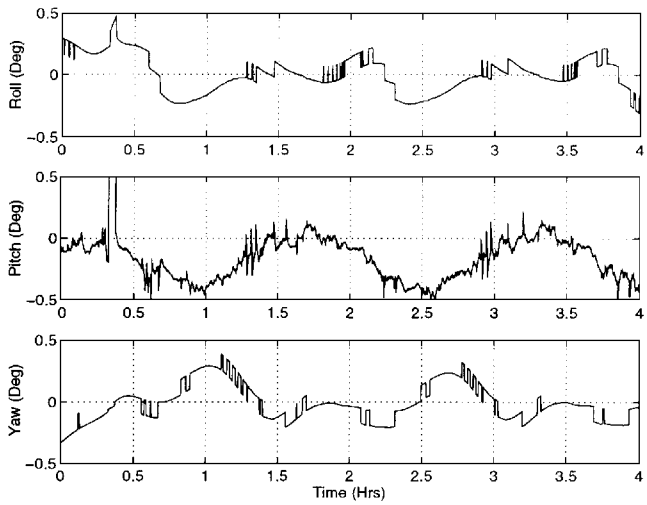


**Fig. 4 Plot of attitude errors between TRIAD solution and MME magnetometer-only solution.**

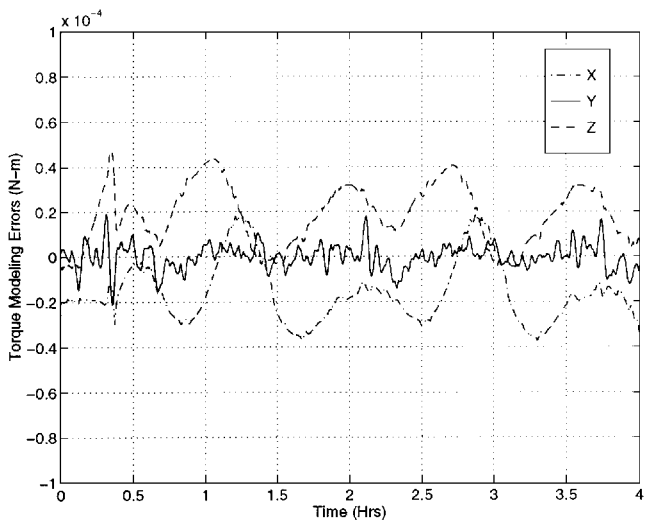


**Fig. 5 Plot of MME-determined torque modeling errors.**

Finally, the MME estimator is used to estimate the torque modeling error using Eq. (53). This is important for purposes of updating the dynamics model using linear or nonlinear identification techniques.[21] Because the angular velocity estimates have been significantly smoothed using Eqs. (46–48), the MME estimator for the torque case was implemented with $W = 0$, so that the estimated angular momentum matches the measured angular momentum exactly for any $R$. Therefore, no tuning of the MME estimator parameters is required. Also, no modeling of disturbance torques or control torques is used in the MME estimator, i.e., $N = \mathbf{0}$. A plot of the determined torque modeling errors is shown in Fig. 5. This corresponds to the torque modeling errors determined using the full nonlinear solution of the TPBVP shown in Eqs. (21) and (23). Therefore, the linearized MME approach provides accurate solutions without using computationally expensive methods, such as a gradient search, for the full nonlinear solution. Also, the MME estimator is able to easily estimate the required torque error using no modeling of disturbance torques, unlike a Kalman filter, which required extensive modeling of disturbance torques (used in $N$) and intensive tuning of filter parameters.[16]

## Conclusions

An MME algorithm is presented for use in attitude estimation. This algorithm was developed for spacecraft that do not possess angular rate sensing equipment. A general form of the optimal estimation approach is shown that involves a nonlinear two-point-boundary-value problem, which can be solved only by use of computationally intense methods. A linearized solution also is shown

that is more efficient than methods that solve the general form. Both solutions can determine the torque modeling-error input in the dynamics equation, which may be used for identification purposes. The MME-based attitude estimator then was applied to determine the attitude of an actual spacecraft. Results indicated that an MME-based approach provides a viable approach that can be used to determine the attitude of a spacecraft from magnetometer measurements only, while providing substantial smoothing of noisy measurement data.

## Acknowledgments

The first author's work was supported by a National Research Council Postdoctoral Fellowship tenured at NASA Goddard Space Flight Center. The author greatly appreciates this support. Also, this author wishes to thank D. Joseph Mook for the many comments and suggestions made throughout this work.

## References

[1]Lerner, G. M., "Three-Axis Attitude Determination," *Spacecraft Attitude Determination and Control*, edited by J. R. Wertz, Reidel, Dordrecht, The Netherlands, 1978, pp. 420–428.

[2]Shuster, M. D., and Oh, S. D., "Attitude Determination from Vector Observations," *Journal of Guidance and Control*, Vol. 4, No. 1, 1981, pp. 70–77.

[3]Markley, F. L., "Attitude Determination from Vector Observations: A Fast Optimal Matrix Algorithm," *Journal of the Astronautical Sciences*, Vol. 41, No. 2, 1993, pp. 261–280.

[4]Wahba, G., "A Least-Squares Estimate of Satellite Attitude," *SIAM Review*, Vol. 7, No. 3, 1965, p. 409 (Problem 65-1).

[5]Kalman, R. E., "A New Approach to Linear Filtering and Prediction Problems," *Journal of Basic Engineering*, Vol. 82, March 1962, pp. 34–45.

[6]Gelb, A., *Applied Optimal Estimation*, MIT Press, Cambridge, MA, 1974, Chap. 1.

[7]Pauling, D. C., Jackson, D. B., and Brown, C. D., "SPARS Algorithms and Simulation Results," *Proceedings of the Symposium on Spacecraft Attitude Determination*, Vol. 1, 1969, pp. 293–317 [Aerospace Corp., Rept. TR-0066(5306)-12].

[8]Toda, N. F., Heiss, J. L., and Schlee, F. H., "SPARS: The System, Algorithms, and Test Results," *Proceedings of the Symposium on Spacecraft Attitude Determination*, Vol. 1, 1969, pp. 361–370 [Aerospace Corp., Rept. TR-0066(5306)-12].

[9]Shuster, M. D., "A Survey of Attitude Representations," *Journal of the Astronautical Sciences*, Vol. 41, No. 4, 1993, pp. 439–517.

[10]Lefferts, E. J., Markley, F. L., and Shuster, M. D., "Kalman Filtering for Spacecraft Attitude Estimation," *Journal of Guidance, Control, and Dynamics*, Vol. 5, No. 5, 1982, pp. 417–429.

[11]Chu, D., and Harvie, E., "Accuracy of the ERBS Definitive Attitude Determination System in the Presence of Propagation Noise," *Proceedings of the Flight Mechanics/Estimation Theory Symposium*, NASA Goddard Space Flight Center, Greenbelt, MD, 1990, pp. 97–114.

[12]Bar-Itzhack, I. Y., and Deutschmann, J. K., "Extended Kalman Filter for Attitude Estimation of the Earth Radiation Budget Satellite," *Proceedings of the AAS Astrodynamics Conference* (Portland, OR), 1990, pp. 786–796 (AAS Paper 90-2964).

[13]Garrick, J., "Upper Atmospheric Research Satellite (UARS) Onboard Attitude Determination Using a Kalman Filter," *Proceedings of the Flight Mechanics/Estimation Theory Symposium*, NASA Goddard Space Flight Center, Greenbelt, MD, 1992, pp. 471–481.

[14]Sedlack, J., "Comparison of Kalman Filter and Optimal Smoother Estimates of Spacecraft Attitude," *Proceedings of the Flight Mechanics/Estimation Theory Symposium*, NASA Goddard Space Flight Center, Greenbelt, MD, 1992, pp. 431–445.

[15]Challa, M. S., Natanson, G. A., Baker, D. E., and Deutschmann, J. K., "Advantages of Estimating Rate Corrections During Dynamic Propagation of Spacecraft Rates—Applications to Real-Time Attitude Determination of SAMPEX," *Proceedings of the Flight Mechanics/Estimation Theory Symposium*, NASA Goddard Space Flight Center, Greenbelt, MD, 1994, pp. 481–495.

[16]Challa, M. S., "Solar, Anomalous, and Magnetospheric Particle Explorer (SAMPEX) Real-Time Sequential Filter (RTSF)," NASA Goddard Space Flight Center, Evaluation Rept., Greenbelt, MD, April 1993.

[17]Mook, D. J., and Junkins, J. L., "Minimum Model Error Estimation for Poorly Modeled Dynamic Systems," *Journal of Guidance, Control, and Dynamics*, Vol. 3, No. 4, 1988, pp. 367–375.

[18]Stry, G. I., and Mook, D. J., "An Analog Experimental Study of Nonlinear Identification," *Nonlinear Dynamics*, Vol. 3, No. 1, 1992, pp. 1–11.

[19]McPartland, M. D., and Mook, D. J., "Nonlinear Model Identification of Electrically Stimulated Muscle," *Proceedings of the IFAC Symposium on Modeling and Control in Biomedical Engineering* (Galveston, TX), 1994, pp. 23, 24.

[20]Mook, D. J., "Robust Attitude Determination Without Rate Gyros," *Proceedings of the AAS/GSFC International Symposium on Space Flight Dynamics*, NASA Goddard Space Flight Center, Greenbelt, MD, 1993, AAS Paper 93-299.

[21]DePena, J., Crassidis, J. L., McPartland, M. D., Meyer, T. J., and Mook, D. J., "MME-Based Attitude Dynamics Identification and Estimation for SAMPEX," *Proceedings of the Flight Mechanics/Estimation Theory Symposium*, NASA Goddard Space Flight Center, Greenbelt, MD, 1994, pp. 497–512.

[22]Crassidis, J. L., and Markley, F. L., "An MME-Based Attitude Estimator Using Vector Observations," *Proceedings of the Flight Mechanics/Estimation Theory Symposium*, NASA Goddard Space Flight Center, Greenbelt, MD, 1995, pp. 137–151.

[23]Markley, F. L., "Equations of Motion," *Spacecraft Attitude Determination and Control*, edited by J. R. Wertz, Reidel, Dordrecht, The Netherlands, 1978, pp. 510–523.

[24]Freund, J. E., and Walpole, R. E., *Mathematical Statistics*, Prentice–Hall, Englewood Cliffs, NJ, 1987, Chap. 8.

[25]Crassidis, J. L., Mason, P. A. C., and Mook, D. J., "Riccati Solution for the Minimum Model Error Algorithm," *Journal of Guidance, Control, and Dynamics*, Vol. 16, No. 6, 1993, pp. 1181–1183.

[26]Flatley, T. W., Forden, J. K., Henretty, D. A., Lightsey, E. G., and Markley, F. L., "On-board Attitude Determination and Control for SAMPEX," *Proceedings of the Flight Mechanics/Estimation Theory Symposium*, NASA Goddard Space Flight Center, Greenbelt, MD, 1990, pp. 379–398.